

Analyses of the impact of climate change on water resources components, drought and wheat yield in semiarid regions: Karkheh River Basin in Iran

S. Ashraf Vaghefi,¹ S. J. Mousavi,¹ K. C. Abbaspour,^{2*} R. Srinivasan³ and H. Yang²

¹ Department of Civil and Environmental Engineering, Amirkabir University of Technology, Tehran, Iran

² Eawag, Swiss Federal Institute of Aquatic Science and Technology, PO Box 611, 8600, Dübendorf, Switzerland

³ Texas A&M University, Texas Agricultural Experimental Station, Spatial Science Lab, College Station, TX, 77845, USA

Abstract:

Water resources availability in the semiarid regions of Iran has experienced severe reduction because of increasing water use and lengthening of dry periods. To better manage this resource, we investigated the impact of climate change on water resources and wheat yield in the Karkheh River Basin (KRB) in the semiarid region of Iran. Future climate scenarios for 2020–2040 were generated from the Canadian Global Coupled Model for scenarios A1B, B1 and A2. We constructed a hydrological model of KRB using the Soil and Water Assessment Tool to project water resources availability. Blue and green water components were modeled with uncertainty ranges for both historic and future data. The Sequential Uncertainty Fitting Version 2 was used with parallel processing option to calibrate the model based on river discharge and wheat yield. Furthermore, a newly developed program called *critical continuous day calculator* was used to determine the frequency and length of critical periods for precipitation, maximum temperature and soil moisture. We found that in the northern part of KRB, freshwater availability will increase from 1716 to 2670 m³/capita/year despite an increase of 28% in the population in 2025 in the B1 scenario. In the southern part, where much of the agricultural lands are located, the freshwater availability will on the average decrease by 44%. The long-term average irrigated wheat yield, however, will increase in the south by 1.2%–21% in different subbasins; but for rain-fed wheat, this variation is from –4% to 38%. The results of critical continuous day calculator showed an increase of up to 25% in both frequency and length of dry periods in south Karkheh, whereas increasing flood events could be expected in the northern and western parts of the region. In general, there is variability in the impact of climate change in the region where some areas will experience net negative whereas other areas will experience a net positive impact. Copyright © 2013 John Wiley & Sons, Ltd.

KEY WORDS SWAT; critical continuous day calculator; SWAT-CUP; wheat yield; parallel SUFI-2

Received 11 April 2012; Accepted 28 January 2013

INTRODUCTION

Climate change is associated with shifts in mean climate conditions and more severe extreme weather conditions (Easterling *et al.*, 2000). Observational evidence from all continents and most oceans shows that natural systems are being affected by regional climate changes; particularly, temperature increases (IPCC, 2007; Mishra and Singh, 2011). Previous studies (e.g. Vörösmarty *et al.*, 2000; Abbaspour *et al.*, 2009; Beyene *et al.*, 2010; Xiao *et al.*, 2010; Setegn *et al.*, 2011; Wang *et al.*, 2011) have shown that climate change would have significant effects on water availability, water stresses and water demand.

The use of hydrological models in planning and management of water resources (Shuol *et al.*, 2008a, 2008b; Faramarzi *et al.*, 2009) and analyses of the impact of climate change on water components (Srinivasan *et al.*, 1998; Milly *et al.*, 2005; Abbaspour *et al.*, 2009) has become a norm recently. In particular blue water, green water storage and green water flow (Falkenmark and

Rockström, 2006) have been quantified in different parts of the world including Africa (Shuol *et al.*, 2008b) and Iran (Faramarzi *et al.*, 2009). Blue water is the water that could be directly used to meet various demands such as irrigation, urban and industrial use. It comprises of water in rivers and aquifers. Green water flow is the evapotranspiration and green water storage is the soil water, which is the source of rain-fed agriculture.

Crop production is affected by meteorological variables, including rising temperatures, changing precipitation regimes and increased atmospheric carbon dioxide levels (Adams *et al.*, 1998). The impact of climate change on agricultural production varies through time and space and is positive in some agricultural systems and regions while negative in others. Liu *et al.* (2009) showed 7%–27% increase in millet, 5%–7% increase in rice and 3%–4% increases in maize yields in Sub-Saharan Africa, whereas Tao *et al.* (2009) reported decreases of 9.7%, 15.7% and 24.7% in maize yield in Henan province of China during the 2020s, the 2050s and the 2080s, respectively.

Water resources in Iran have in recent years experienced increasing pressures from rising demands and recurrent droughts. The situation is particularly severe in semiarid regions (Ahmad and Giordano, 2010). In the

*Correspondence to: Karim Abbaspour, Eawag, Ueberlandstr 133, 8600 Dübendorf, Switzerland, Tel: +41 58 7653359, Fax: +41 58 7653375
E-mail: abbaspour@eawag.ch

semiarid province of Khuzestan, where the southern part of the Basin is located, rivers Karkheh, Karun and Marun have decreased in discharge by 49%, 37% and 40%, respectively, in 2000–2001 as compared with the average of the past 32 years (Mousavi, 2005). Improving water resources management and water use efficiency in the semiarid regions is of importance to sustain the agricultural and industrial developments. Karkheh River Basin (KRB) is among the initially nine globally distributed watersheds selected by the CGIAR Challenge Program for increasing water productivity of agriculture (Farahani and Oweis, 2008). The importance of analyzing the impact of land use and climate changes on water quality, water resources and water demands in KRB has been emphasized in previous studies (Ahmad *et al.*, 2009; Marjanizadeh *et al.*, 2010; Masih *et al.*, 2010; Salajegheh *et al.*, 2011). These studies emphasize different aspects of water issues separately. To better manage the water resources of KRB in the coming years, we took a holistic look at water resources and analyzed the impact of climate change on different components of water balance, drought and crop yield.

The main objectives of this work were (i) to investigate the impact of climate change on both water resources (blue water, green water flow and green water storage) and crop yield, especially winter wheat for 2020–2040 and compare it with the historical data (1985–2005), and (ii) to study the variation in the length and frequency of dry periods in both historical and future times. The program Soil and Water Assessment Tool (SWAT) (Arnold *et al.*, 1998) was used to model the hydrology and crop production of KRB. The SWAT model in this study was calibrated and validated using the parallel Sequential Uncertainty Fitting Version 2 (SUFI-2) in the SWAT-CUP software (Abbaspour *et al.*, 2004, 2007; Rouhollahnejad *et al.*, 2012)

MATERIALS AND METHODS

The Karkheh River Basin

The KRB (approximately 51,000 km²) stretches from the Zagros Mountains to the Hoor-Al-Azim Swamp, which is a trans-boundary wetland located at the Iran–Iraq border. The river basin is located in the southwestern part of Iran, between 30°N to 35°N and 46°E to 49°E. The basin is one of the most productive agricultural areas in Iran (Figure 1). It covers 9% of Iran's irrigated area and produces 10%–11% of the country's wheat. The KRB is known as the “food basket of Iran” (Ahmad and Giordano, 2010). The elevation of the basin ranges from less than 10 m above sea level in the southern areas to more than 3500 m in the hilly parts of the basin. The southern part of the Basin receives an average annual precipitation of approximately 250 mm/year, whereas the northern part receives up to 700 mm/year. Precipitation in many areas is generally insufficient to meet crop water requirements, and therefore irrigated agriculture is important in the basin (Keshavarz *et al.*, 2005; Ahmad

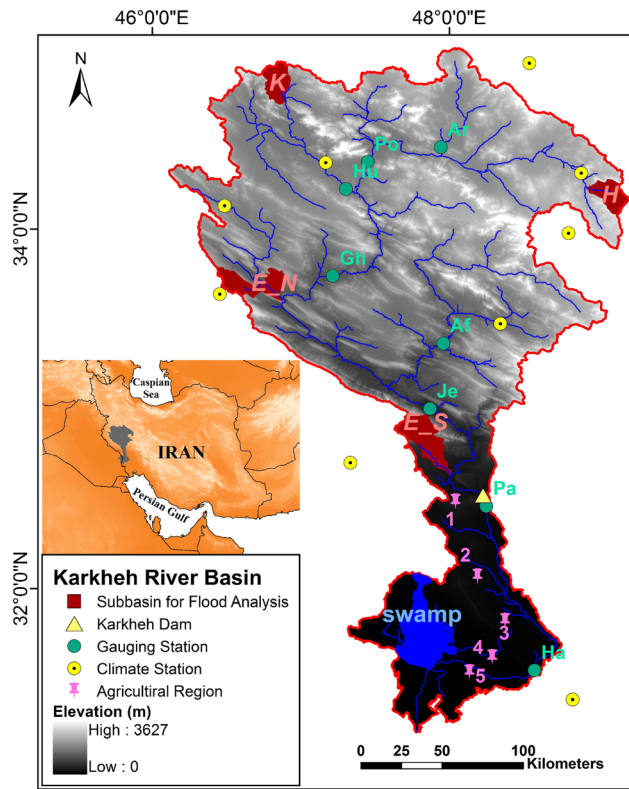


Figure 1. Study area location in Iran showing the five important agricultural regions—(1) Dashte Abbas, (2) Dolsagh, (3) Arayez, (4) Hamidiyeh and (5) Azadegan, and river discharge stations—Aran (Ar), Polchehr (Po), Ghurbagh (Gh), Huliyan (Hu), Afarine (Af), Jelogir (Je), Pay-e-Pol (Pa), Hamidiyeh (Ha) and the regions of Kordestan (K), Hamedan (H), Eilam North part (E_N), Eilam South part (E_S) where the climate change impact is highlighted

et al., 2009). There are five major agricultural regions in the southern part of the Basin (Lower Karkheh) (Figure 1) dominated by winter wheat. The yields of winter wheat in the different regions are given in Table I. In all regions, more than 50% of agricultural land is wheat. Starting dates of cropping for wheat in agricultural regions spatially varies from 20 September to 10 October and harvest dates varies from 20 May to 10 June.

The SWAT simulator

The SWAT model has been developed to quantify the impact of land management practices in large and complex watersheds. SWAT simulates the hydrology of a watershed in two separate components. One is the land phase of the hydrological cycle and the other is routing phase of hydrologic cycle. The first controls the amount of water, sediment, nutrient and pesticide loadings to the main channel in each subbasin, and the second defines the movement of water, sediments, nutrients and organic chemicals through the channel network of the watershed to the outlet. A water balance model is simulated in the land component of SWAT (Arnold *et al.*, 1998, 1999; Gassman *et al.*, 2007). SWAT subbasin components consist of hydrology, weather, sedimentation, crop growth, nutrients, pesticides and agricultural management. Hydrological processes include simulation of surface runoff, percolation, lateral flow and flow from shallow aquifers to streams, potential evapotranspiration, snowmelt, transmission losses

Table I. Percentage distribution of winter wheat in the current crop pattern for five important agricultural regions located in the southern part of the KRB (mostly downstream of Karkheh Dam) (Mahab Ghods Consulting Engineer Co, 2009).

Agricultural region	Distribution of winter wheat in the current crop pattern (%)	Total winter wheat area (ha)	Area of irrigated winter wheat (ha)	Area of rain-fed winter wheat (ha)
Dashte Abbas (1) ^a	59.5	11,320	9,720	1500
Dolsagh (2)	58.7	9,470	3,890	3150
Arayez (3)	59.1	17,080	11,200	5880
Hamidiyeh (4)	75.3	12,840	12,840	—
Azadegan (5)	70.4	50,050	50,050	—

^a The number in brackets identify the regions in the map.

from streams and water storage and losses from ponds. SWAT is a continuous simulation model, which operates on a daily time step (Neitsch *et al.*, 2002).

Climate change model and scenarios

In this study, we used the Coupled Global Climate Model (CGCM3.1) (version T63) of the Canadian Centre for Climate Modeling and Analysis. This version has surface grid with latitude/longitude resolution of 2.8° and 31 vertical levels. A key aspect of the climate change impact study is the spatial and temporal downscaling of the GCM results. In this study, the CGCM data were downscaled using the nearest observation station for the period of 1980–2002 in the KRB. With this specification, four grid points were within our study site. For rainfall, we used a simple ratio method, in which for each month, we divided the average CGCM data by the observed data and multiplied the daily CGCM data by this factor to obtain future daily rainfall data. For the temperature, we tested linear and nonlinear models as described by Wilby and Wigley (1997) and chose a fourth-degree regression model. In general, the results of a first-degree linear and a fourth-degree nonlinear models were similar except for small and large temperature values, where the nonlinear model performed systematically better as also reported by Abbaspour *et al.* (2009).

Future climate scenarios for periods of 2020–2040 were generated from CGCM for scenarios A1B, B1 and A2 (IPCC, 2000). The A1B scenario describes a future world of very rapid economic growth, global population that peaks in the midcentury and declines thereafter and the rapid introduction of new and more efficient technologies. Major underlying themes are convergence among regions, capacity building and increased cultural and social interactions, with a substantial reduction in regional differences in per capita income. The A2 scenario describes a very heterogeneous world. The underlying theme is self-reliance and preservation of local identities. Fertility patterns across regions converge very slowly, which results in continuously increasing global population. Economic development is primarily regionally oriented, and per capita economic growth and technological changes are more fragmented and slower than in other storylines. The B1 scenario describes a convergent world with the same global population that peaks in midcentury and declines thereafter, as in the A1B, but with rapid changes in economic structures toward a service and information economy, with reductions in

material intensity, and the introduction of clean and resource-efficient technologies.

The impact of climate change was quantified as the percent differences between the predictions calculated at the 50% probability level for future years and averaged over the period of 2020–2040. For historical data, the averaging was performed for the period of 1985–2005. In addition, the impact of climate change on the frequency and length and the shift in the start and end of the dry periods were calculated. The latter were calculated using a critical continuous day calculator (CCDC) as described in the next section.

Calibration, validation and uncertainty analysis

The SUFI-2 algorithm maps all uncertainties (parameter, conceptual model, input, etc.) on the parameter ranges and tries to capture most of the measured data within the 95% prediction uncertainty (95PPU) calculated at the 2.5% and 97.5% levels of the cumulative distribution of an output variable obtained through Latin hypercube sampling. The goodness of fit and the degree to which the calibrated model accounts for the uncertainties are assessed by two indices: *R* factor and *P* factor. The *P* factor is a fraction of measured data bracketed by the 95PPU band. The *P* factor varies from 0 to 1, where 1 is the highest value, that is, 100% bracketing of the measured data. The *R* factor is the average width of the 95PPU band divided by the standard deviation of the measured variable. A value less than 1 is reported to be desirable for this parameter (Abbaspour *et al.*, 2004, 2009). These two indices can be used to judge the strength of the calibration. A larger *P* factor can be achieved at the expense of a larger *R* factor. Hence, often a balance must be reached between the two. When acceptable values of *R* and *P* factors are reached, then the parameter uncertainties are the calibrated parameter ranges. SUFI-2 allows usage of different objective functions such as R^2 or Nash–Sutcliffe efficiency (NSE) (Nash and Sutcliffe, 1970). In this study, we used NSE and PBIAS (Moriassi *et al.* 2007) for discharge and root mean square error for crop yield (Faramarzi *et al.* 2010a).

Critical continuous day calculator

We developed a program called CCDC (downloadable from www.swatcupiran.com) to calculate the number of events of continuous days where precipitation, soil moisture and maximum temperature meet certain constraints with

respect to the number of days and given critical values. For example, a dry period for maximum temperature is defined as a period of >120 continuous days where maximum temperature is >30°C. For precipitation, a dry period is a period of >120 continuous days when rainfall is <2 mm day⁻¹. A dry period is also defined for soil moisture when it remains <2% in the soil profile for >120 continuous days. The numbers are chosen subjectively here as an example and could differ for different regions. We used these numbers to indicate little rainfall or a dry period (Byun and Wilhite, 1999). The CCDC program uses SWAT's output file (output.hru) and SWATCUP's output file (95ppu.txt) as inputs.

Model setup

Basic SWAT input data included soil map obtained from the global map of the Food and Agriculture Organization of the United Nations (FAO, 1995), which provides data for 5000 soil types comprising two layers (0–30 and 30–100 cm depth) at a spatial resolution of 10 km. Further data on soil physical properties required for SWAT were obtained from Schuol *et al.* (2008a). Land use map with a resolution of 900 m was obtained from Mahab Ghods Consulting Engineers Co. Digital elevation model at a 90-m resolution was provided by SRTM of NASA (Jarvis *et al.*, 2008). The river map of major local rivers was from Iran Water & Power Resources Development Co (2010). Climate data from nine climate stations were obtained from Iranian Ministry of Energy. Crop and agricultural management data were provided by the Mahab Ghods Consulting Engineers Co. The Karkheh reservoir was also included in the model with reservoir operational information starting from 2000 when it became operational for the first time provided by the Ministry of Energy (1998). We considered management information such as minimum and maximum daily outflow for the month, reservoir surface area when the reservoir is filed to the emergency and principal spillway, volume of the water needed to fill the reservoir to the emergency and principal spillway. Monthly discharge data for eight river gauges were provided by the local water authorities (Figure 1).

Observed monthly discharge and winter wheat yield were used for model calibration (1989–2005) and validation (1982–1988). The selection of parameters to calibrate was based on sensitivity analysis and previous studies (Abbaspour *et al.*, 2007; Schuol *et al.*, 2008a; Faramarzi *et al.*, 2009). On the basis of this, 26 SWAT parameters were selected for model calibration for both discharge (20 parameters) and crop yield (6 parameters). The parallel SUFI-2 (Rouhollahnejad *et al.*, 2012) in SWAT-CUP software was used for sensitivity analysis, calibration and uncertainty quantification.

RESULTS AND DISCUSSION

Sensitivity analysis

Eight crop and discharge parameters were found to be sensitive in this study (Table II). Parameters are described

Table II. Sensitive SWAT parameters included in the final calibration, their initial and final ranges and their t and P values

Parameter name	Definition	t	P	Initial range	Final range
v__HEAT-UNITS	Crop required heat units (irrigated)	11.3	5.64×10^{-24}	1500 to 3000	2300 to 2800
v__HI	Harvest index (irrigated)	9.7	2.36×10^{-24}	0 to 1	0.45 to 0.63
r__CN2.mgt	SCS runoff curve number	7.7	2×10^{-13}	-0.5 to 0.5	-0.15 to 0.05
r__CN2.mgt	SCS runoff curve number	6.2	5×10^{-9}	-0.5 to 0.5	-0.1 to 0.05
46_52,54,56,58,60,70,73					
v__CH N2.rte	Manning's n value for main channel	3.4	0.000828	0 to 0.3	0.11 to 0.23
v__ALPHA BF.gw	Baseflow alpha factor (days)	-2.9	0.004329	0 to 1	0 to 0.511
r__SOL BD.sol	Soil bulk density ($g\ cm^{-3}$)	2.5	0.011557	-0.5 to 0.5	-0.2 to 0.25
v__GW REVAP.gw	Groundwater revap (Water in shallow aquifer returning to root zone) coefficient	1.8	0.0728	0.02 to 0.2	0.094 to 0.2
v__GWQMN.gw	Threshold depth of water in the shallow aquifer required for return flow to occur (mm)	-1.9	0.05658	0 to 5000	0 to 3064.7
v__SMFMX.bsn	Maximum melt rate for snow during the year ($mm\ C^{-1}\ day^{-1}$)	-1.7	0.09758	0 to 10	0 to 6.587
r__OVN.hru	Manning's n value for overland flow	-1.4	0.157168	-1 to 1	-0.2 to 0.0
r__OVN.hru	Manning's n value for overland flow	-1.0	0.257168	-1 to 1	-0.25 to 0.05
v__HEAT-UNITS	Crop required heat units (rain fed)	1.0	0.315	1400 to 2500	1500 to 2000
v__HI	Harvest index (rain fed)	1.0	0.359	0 to 1	0.35 to 0.45

in terms of their parameterization characteristics, which are defined as the regionalization based on different soils, land uses, management or locations within the watershed. In this study, we parameterized CN2, OV_N, SOL_AWC and HEAT_UNITS (abbreviations are explained in Table II) for irrigated and rain-fed regions, as well as the HI based on their location in the watershed by assigning the subbasin numbers to the parameter. For more details on parameterization, see the SWAT-CUP manual (Abbaspour, 2011).

As expected from the literature, CN2 was the most sensitive parameter for discharge followed by CH_N2. For winter wheat, the most sensitive parameter was HEAT-UNITS followed by HI.

Discharge

Station Pay-e-Pol, downstream of Karkheh Dam, has an important role in irrigation of agricultural plains. Results of the model performance are given in terms of *P* factor and *R* factor indices for both calibration and validation periods (Table III). The *P* factor indicates that for all stations, more than 75% of the data are bracketed in the prediction uncertainty of the model, whereas the *R* factors are mostly around or below 1. In general, in the south of Karkheh Dam (Pay-e-Pol and Hamidiyeh stations) (Figure 1), the model prediction has larger uncertainties. This is especially true in Hamidiyeh station, where the *R* factor is 1.42. Hamidiyeh is a region of significant water management where different demand sectors require water transfers from the Karkheh Dam. It has also been shown before that the larger the water management the poorer the model calibration results (Faramarzi *et al.*, 2009). In the north of Karkheh Dam (e.g. Jelogir station), model performance is in general better and uncertainties smaller mainly due to lesser water management practices. On the basis of the NSE and PBIAS statistics (Table III), the discharge simulation can be judged as satisfactory according to criteria given by Moriasi *et al.* (2007).

The parallel processing option of SWAT-CUP speeded up the calibration process by reducing the total time from approximately 8 days to about half a day.

Winter wheat

Observed yields are generally inside or quite close to predicted yield bands for both rain-fed and irrigated agriculture (Figure 2). In irrigated plains, the yield varies from 2050 to 3320 kg ha⁻¹, with the highest yield found in the Azadegan (2002) region and the lowest in the Dashte Abbas (1990). For the rain-fed areas, the lowest yield belongs to the Arayez region (440 kg ha⁻¹ in 1996) and the highest to Dolsagh region (870 kg ha⁻¹ in 1992). For the irrigated yield, the *P* factors are generally larger than 0.78 for calibration and vary from 0.73 to 0.76 for the validation period (Table IV). The *R* factor values are quite small, indicating low prediction uncertainties. For the rain-fed production, the uncertainties are larger than the irrigated yield as indicated by generally larger *R* factor values. This is because of the year-to-year climatic variation in the rain-fed yield, which is also incorporated in the 95PPU band.

Impact of climate change on water resources

The availability of the historical renewable fresh-water resources in the KRB is approximately 908 m³/(capita year) based on the population of 2002, which was 3.5 million (Ahmad and Giordano, 2010). The estimated future quantity is approximately 1662 m³/capita/year for the population of 2025, which is estimated to be 4.5 million (Marjanizadeh *et al.* 2010) based on the A2 climate scenario. In this study, we found that in the northern part, the fresh water availability increases from 1716 to 2670 m³/capita/year in the same period as above; and in the south, the water availability decreases significantly from 740 to 410 m³/capita/year. Although Yang *et al.* (2003) reported a decrease in water availability for Iran to below the water scarcity threshold of 1500 m³/(capita year) by 2030, taking the spatial variability in the climate change into account, the water resources may actually increase in many parts of the country (Abbaspour *et al.*, 2009).

In the middle parts of the basin, a significant increase is seen in precipitation in all climate scenarios (Figures 3a–3d). In the northeast regions, A1B and B1 predict a generally less precipitation; whereas in the northwest, all scenarios predict an increase in precipitation. The production of crops in the

Table III. Calibration (1989–2005) and validation (1982–1988) performance of eight river gauges for discharge

River discharge station	Calibration				Validation			
	<i>P</i> factor	<i>R</i> factor	NSE	PBIAS	<i>P</i> factor	<i>R</i> factor	NSE	PBIAS
Aran (Ar) ^a	0.75	1.02	0.65	-13.1	0.78	1.19	0.53	-17.4
Polchehr (Po)	0.75	1.04	0.79	5.4	0.89	1.24	0.68	9.8
Ghurbagh (Gh)	0.84	0.89	0.66	12.5	0.88	1.11	0.52	14.3
Huliyan (Hu)	0.92	1.08	0.75	8.5	0.94	1.23	0.67	11.2
Afarine (Af)	0.92	1.2	0.63	11.3	0.71	1.28	0.56	15.6
Jelogir (Je)	0.91	1.05	0.74	7.5	0.89	1.13	0.63	9.7
Pay-e-Pol (Pa)	0.83	1.17	0.75	6.9	0.82	1.24	0.59	8.6
Hamidiyeh (Ha)	0.89	1.42	0.59	-18.2	0.97	1.73	0.51	-22.9

^a The abbreviations in brackets identify the river discharge stations in the map

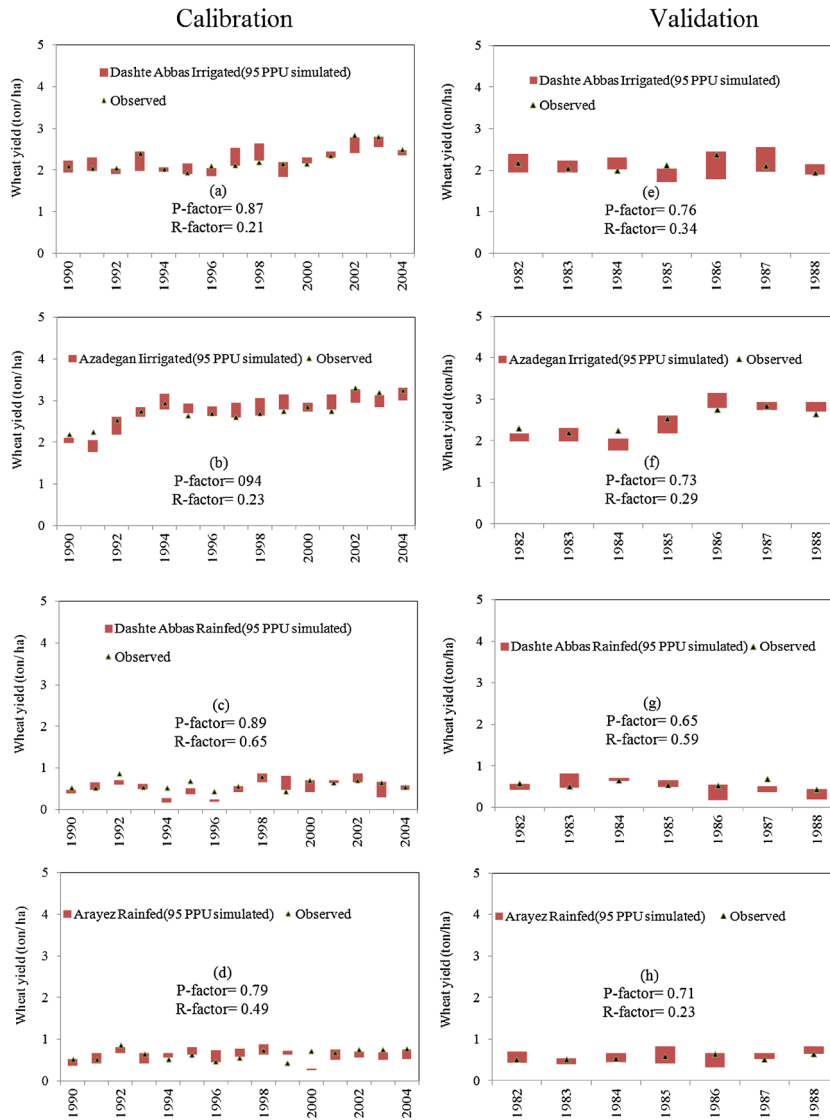


Figure 2. Results of SWAT calibration (left column, 1990–2004) and validation (right column, 1982–1988) for wheat yield (ton ha⁻¹) in selected agricultural regions. (a and e) Dashte Abbas irrigated winter wheat, (b and f) Azadegan irrigated winter wheat, (c and g) Dashte Abbas rain-fed winter wheat and (d and h) Arayez rain-fed winter wheat

Table IV. Calibration (1990–2004) and validation (1982–1988) performance for crop yield in five major agricultural regions (located in the southern part of the KRB mostly downstream of Karkheh dam)

Agricultural region	Calibration (wheat yield)				Validation (wheat yield)			
	<i>P</i> factor	<i>R</i> factor	<i>P</i> factor	<i>R</i> factor	<i>P</i> factor	<i>R</i> factor	<i>P</i> factor	<i>R</i> factor
	Irrigated	Irrigated	Rain fed	Rain fed	Irrigated	Irrigated	Rain fed	Rain fed
Dashte Abbas	0.87	0.21	0.89	0.65	0.76	0.34	0.65	0.59
Dolsagh	0.85	0.39	0.86	0.25	0.75	0.25	0.61	0.31
Arayez	0.83	0.43	0.79	0.49	0.74	0.27	0.71	0.23
Hamidiyeh	0.78	0.29	—	—	0.73	0.36	—	—
Azadegan	0.94	0.23	—	—	0.73	0.29	—	—

southern regions experiences periodic losses as a result of water stresses in the historic period. The predicted 25% decrease in the average rainfall is expected to exasperate the situation. Considering the decrease of precipitation and low economic return of rain-fed agricultural lands in the

lower Karkheh, the necessity to irrigate seems inevitable in the south.

Lower Karkheh experiences the same diurnal temperature as the historic period, except in the western region of Azadegan where temperature differences increase

IMPACT OF CLIMATE CHANGE ON WATER RESOURCES OF KARKHEH RIVER BASIN

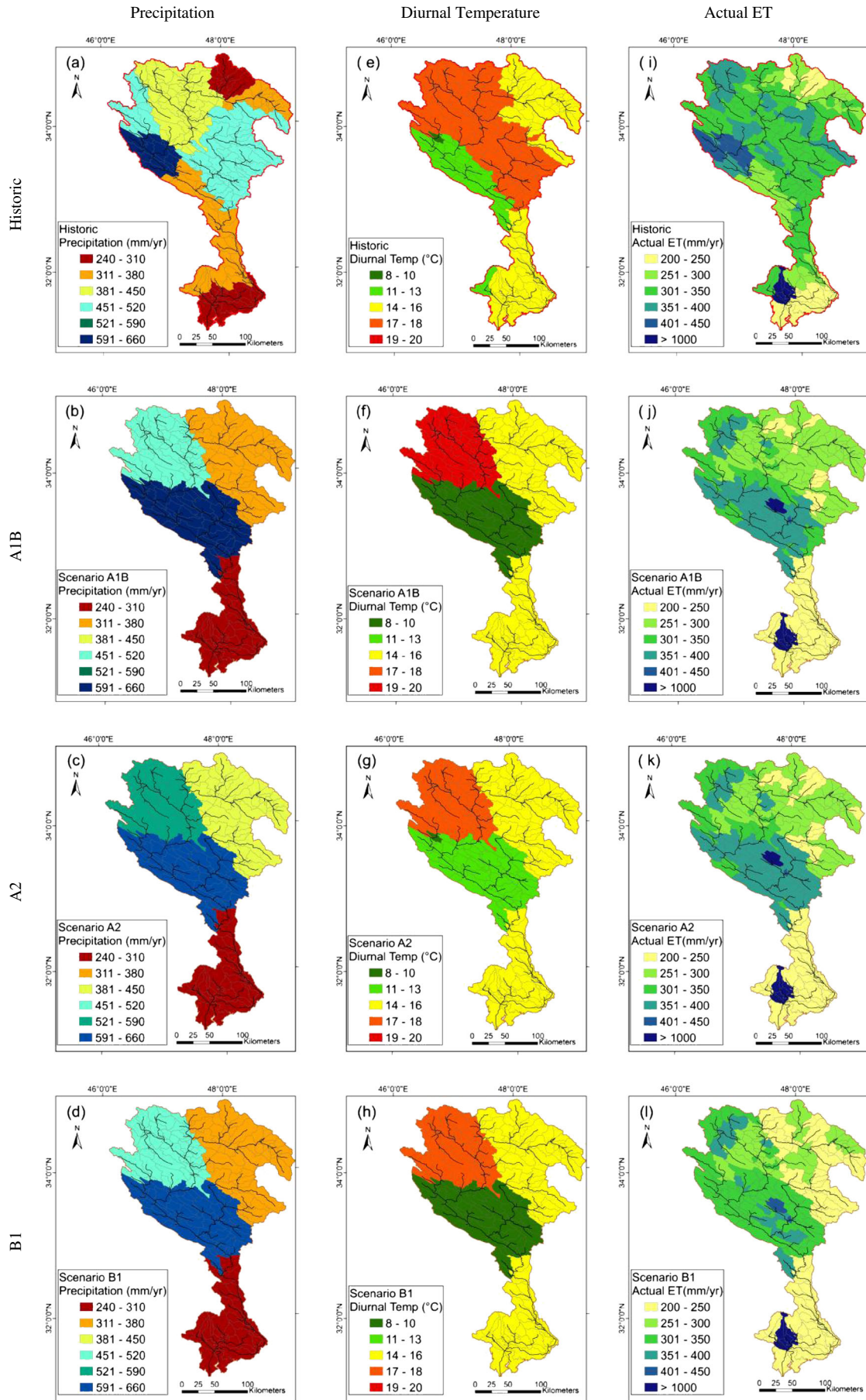


Figure 3. Distribution of (a–d) annual mean of precipitation, (e–h) diurnal temperature range and (i–l) actual evapotranspiration for historic (1985–2005) and future (2020–2040) scenarios

(Figures 3e–3h). The main difference in diurnal temperature appears to be in the midsection of the region, where a 38% decrease is seen in A1B and B1 scenario, whereas A2 predicts a 25% decrease. Some studies show that the declining diurnal temperature may be an indication of beneficial CO₂-induced “global greening” (Myneni *et al.* 1997), which is by definition known to be helping both natural and agro-ecosystems become more productive. A study by Lobell (2007) shows a significant response of cereal yield to diurnal temperature changes.

Historically, the annual ET varies spatially from 230 to 1350 mm, with the highest values found in the Hoor-al-Azim swamp and the lowest in the bare land and desert areas in the southern Karkheh (Figures 3i–3l). The results show similar trend of spatial variation of actual ET with previous studies such as Muthuwatta *et al.*, 2010. All three scenarios indicated changes at the western region of the watershed where a 20% decrease is evident in many subbasins. It also appears that there is less spatial variation in the ET in the central parts of the Karkheh.

Generally, the blue water will increase in the north, east, west and middle parts of KRB (Figures 4a–4d). These increases are more obvious in the western parts, which could have a significant impact on the ecosystem of the region. Those subbasins located in the south of the watershed, especially downstream of Karkheh dam, will not see much change, although in the A2 scenario a little increase is seen in the blue water.

Green water storage in A1B scenario increases by up to 80% in most areas in the northwest part of the Karkheh (Figures 4e–4h). In Dashte Abbas, Dolsagh and Arayez, wherein rain-fed winter wheat is produced, no significant change is seen except for the B1 scenario, under which green water storage decreases from 51–75 to 26–50 mm year⁻¹.

Coefficient of variation (CV) expresses the degree of reliability in blue water resources (Figures 4i–4l). The smaller the CV, the smaller the year-to-year variability of the blue water and the more reliable are the estimates. For the historical period, most parts of the watershed have small CVs, except the Azadegan region in the southern part of the Basin with a CV of larger than 200%. As a result of climate change, there is an increase in CV for A1B and A2 scenarios, which indicate a smaller reliability in the blue water, except the southern parts of the Basin (Azadegan region), where a decrease of CV is seen from an average of 225% to 175%. In the B1 scenario, the CV in blue water becomes more uniform than the historical data as it shows a more uniform interannual variation of blue water.

Impact of climate change on drought and flood events

The subbasins in the northeast of the watershed experience continuous dry days (CCD) with the average of 162 days only four to seven times in the historic period (Figure 5a). This means all subbasins experience the event at least four times, while some subbasins may experience it up to seven times. In the extreme south and the midwestern sections, this frequency increases to 13–14 times (Figure 5a).

In general, the future climate data indicates an increase in the frequency of such dry periods (Figures 5b–5d). The length of such dry periods slightly increases. In the extreme south, increases of up to 201 days are predicted (Figure 5d).

A temperature-based dry period event is defined here as a period of more than 120 consecutive days with maximum temperatures >30°C. The subbasins in the southern part of the Basin experienced 13–16 events with the average length of 165 days in the past 17 years (Figure 5e). In the future, rather small changes are seen in the dry events in B1 and A2, whereas A1B shows the most change in the number of dry periods where increases are seen in the south and north, and middle Basin shows some decreases (Figures 5f–5h).

A critical period is defined in this article as a period (>120 consecutive days) where soil moisture is less than 2% per day in the soil profile. Again, the larger events appear in the southern subbasins where 11–13 times in 20 years the soil moisture is less than the critical value for the average length of 187 days (Figure 5i). This frequency decreases to one to five times in the north, whereas a large number of subbasins experience no such events at all. The impact of climate change is mostly felt in the south, where the frequency of such events increases to 16–18 times in 17 years (Figures 5j–5l).

There appears to be an earlier onset of critical precipitation events in the year, while ending later in the year, indicating longer critical periods for all future scenarios (Figure 6). For the maximum temperature, there is a slight earlier starting, and similar to the precipitation, the periods last longer in the year. The annual variations of dry periods show no critical precipitation and maximum temperature events from 1986 to 1989.

The number of wet days in Kordestan-North (K) (Figure 1) is expected to increase as a result of climate change in all scenarios throughout the year (Figures 8a, 8e and 8i). The increase is the same for precipitation events of ≥ 2 and ≥ 10 mm d⁻¹, but for ≥ 50 mm d⁻¹, there is a substantial increase in the frequency of such rainfall events, especially in the fall. In this region, A2 predicts the largest increase in all rainfall events.

We analyzed the impact of future climate change on floods by calculating the monthly average distribution of the number of wet days with precipitation ≥ 2 , ≥ 10 and ≥ 50 mm d⁻¹ at Kordestan-North (K), Hamedan-North (H), Eilam-North (E_N) and Eilam-South (E_S) across KRB (see Figure 1). Figures 8a–8d show the monthly average number of days with precipitation ≥ 2 mm d⁻¹. It is predicted that in Kordestan-North (Figure 7a) in the Northern part of KRB, the number of wet days will increase as a result of climate change in all scenarios throughout the year. The same increase is more or less for ≥ 10 mm d⁻¹, but for ≥ 50 mm d⁻¹, there is a substantial increase in the frequency of such large rainfall events, especially in the fall. In this region, A2 predicts the largest increase in all rainfall events.

In Hamedan-North, there is an increase in the ≥ 2 -mm d⁻¹ rainfall events throughout the years (Figures 7b, 7f and 7j). However, a decrease is seen in the ≥ 10 -mm d⁻¹

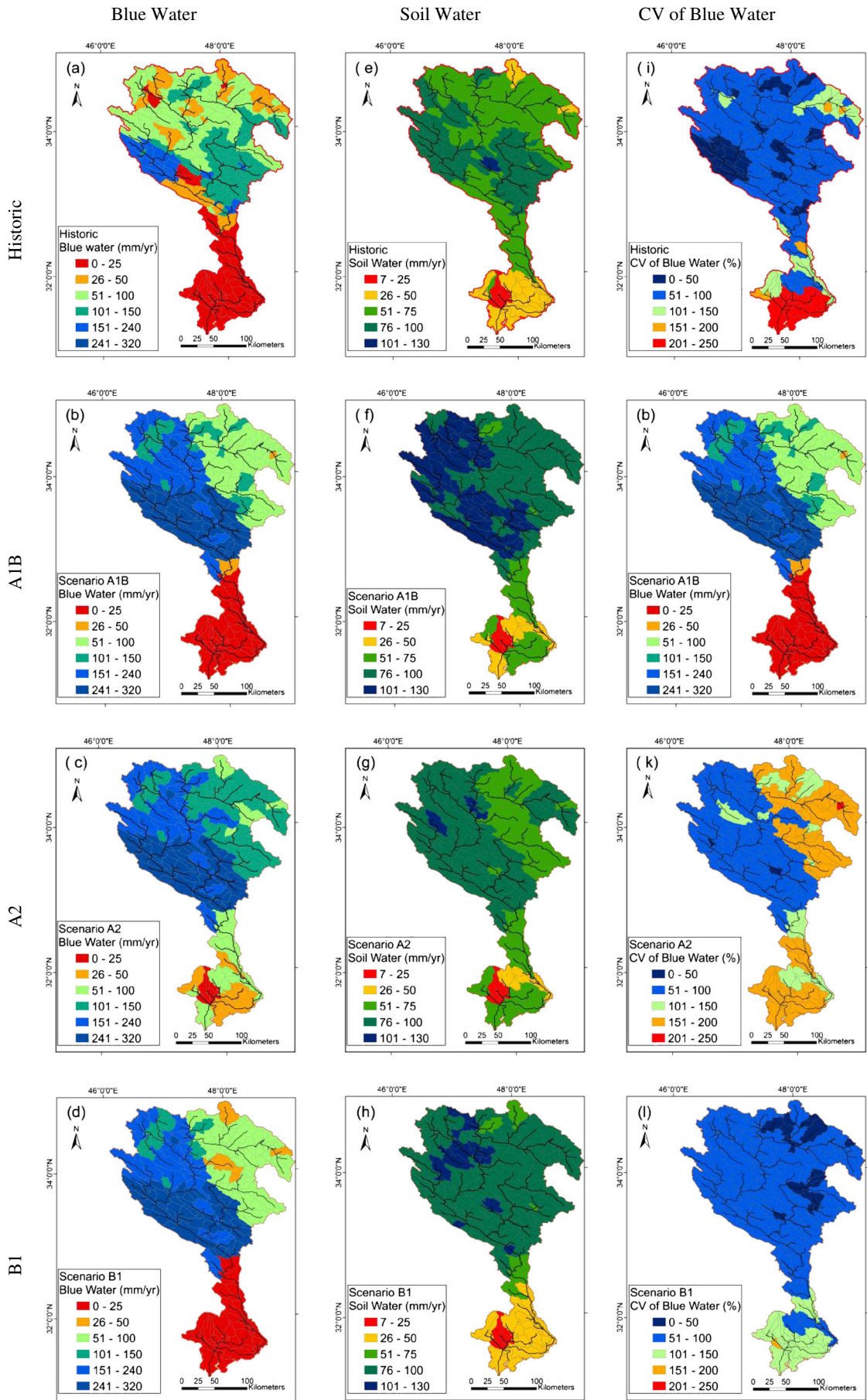


Figure 4. Spatial variation of annually averaged (a–d) blue water (mm yr^{-1}), (e–h) soil water storage (mm yr^{-1}) and (i–l) annual CV for blue water availability for historic (1985–2005) and future (2020–2040) scenarios

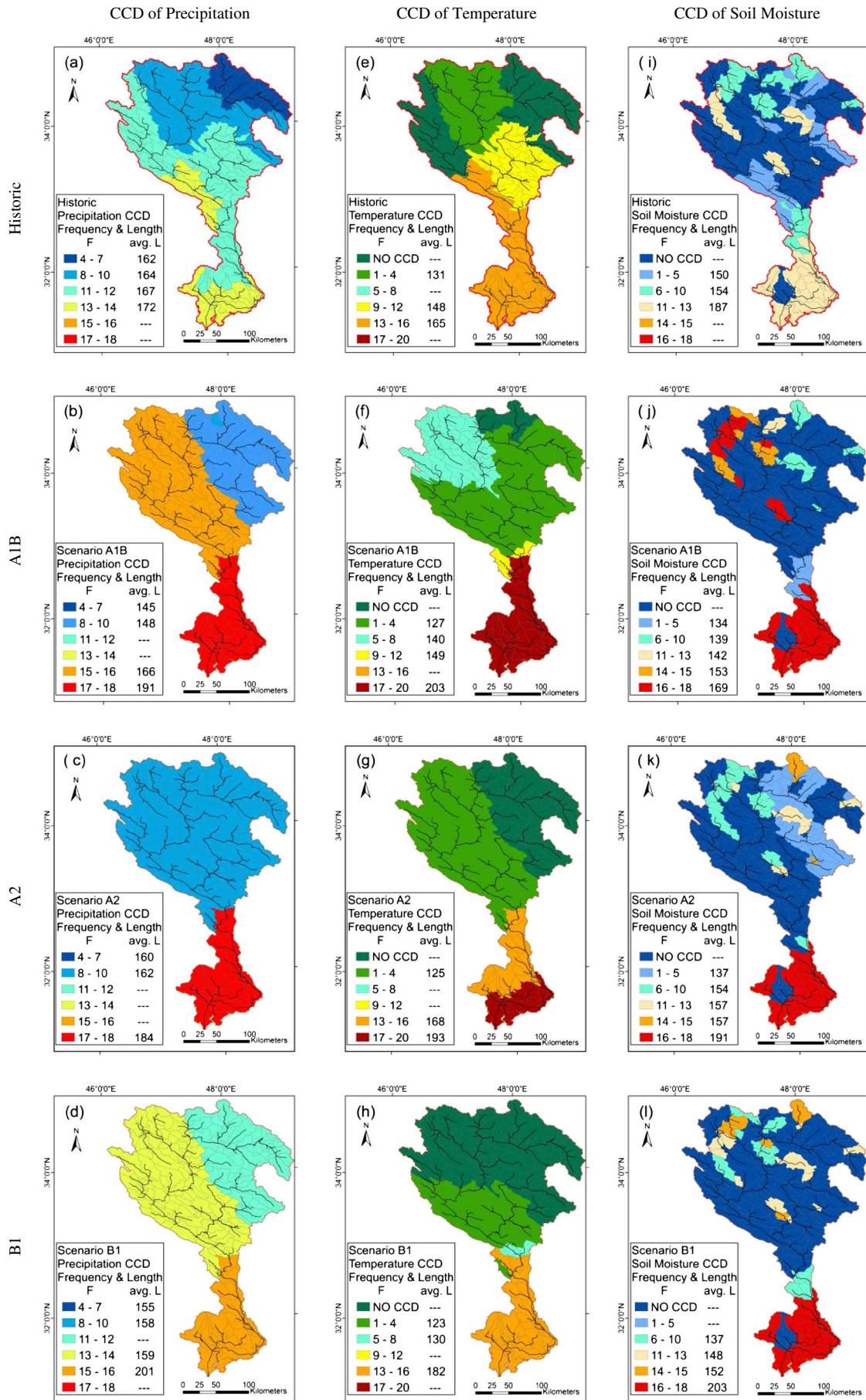


Figure 5. Outputs of the CCDC program. The three columns show the critical continuous days for (a–d) historical and future precipitation, (e–h) maximum temperature and (i–l) soil moisture

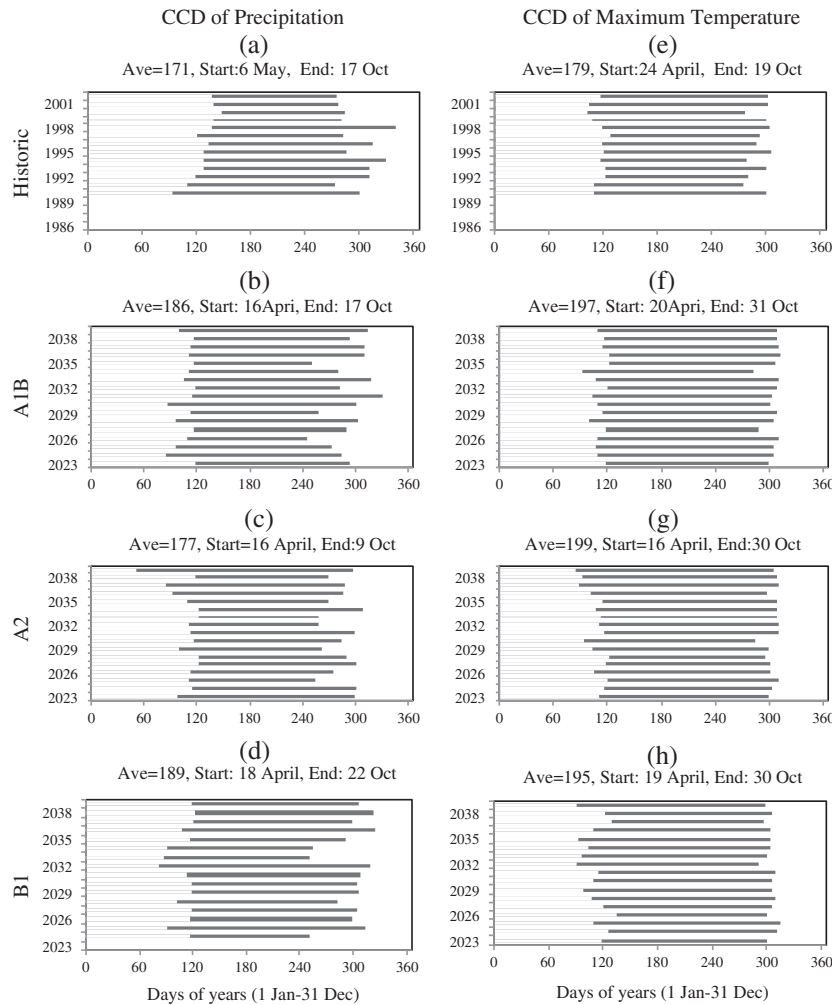


Figure 6. Beginning and ending days of dry periods and average length of the period for precipitation (left column) and temperature (right column). The data are shown for Dashte Abbas for (a and e) historical periods and futures scenarios (b and f) A1B, (c and g) A2 and (d and h) B1

rainfall events from January to May. For the $\geq 50\text{-mm d}^{-1}$ events, which were completely absent in the historical period, an increase is seen in the fall months. Increases in large rainfall events ($\geq 20\text{ mm d}^{-1}$), which happen with less frequency, do not have much impact on water resources but could have devastating effects as they often cause flooding.

In Eilam-North, there is an increase in the $\geq 2\text{-mm d}^{-1}$ rainfall events throughout the year and also for $\geq 10\text{ mm d}^{-1}$ from January to May (Figures 7c, 7g and 7k). This translates into an increase in water resources as shown in the midwestern section of Figure 4. There is also a large increase in the frequency of the $\geq 50\text{-mm d}^{-1}$ events in this region (Figure 7k), which alerts an increasing chance of flooding, especially in the month of October.

Further south in Eilam-South, there is no significant increase in the frequency of different rainfall rates; and in some months, there is even a decrease in the number of rainfall events, especially in February, March and December for the $\geq 2\text{-mm d}^{-1}$ events, and almost throughout the year for the $\geq 10\text{-mm d}^{-1}$ events (Figures 7d, 7h and 7i).

The monthly average river discharge in Kordestan shows an increase (up to 500%) in October for all future scenarios as compared with the historical time (Figure 8a). The most

change in Hamedan is seen in October, especially in the B1 scenario (Figure 8b). In Eilam-North, the same monthly trend as Kordestan is seen, except in July (Figure 8c). In Eilam-South, changes vary from -100% to 50% . In A1B and A2, the most increases are seen in July–August; whereas in the B1 scenario, the most increase is seen in October (Figure 8d). All results show an increasing chance of flooding, especially in the month of October.

In general, the CV of rainfalls $\geq 2\text{ mm d}^{-1}$ decreases, except for a slight increase in Hamedan-North located in the north eastern side of the Basin (Figure 9a). An increase, however, can be seen in the CV of rainfalls $\geq 10\text{ mm d}^{-1}$ (Figure 9b), whereas those of $\geq 50\text{ mm d}^{-1}$ substantially decrease in most parts of the Basin except Eilam-South (Figure 9c). This indicates less consistency in the rainfalls of $\geq 10\text{ mm d}^{-1}$ but a smaller dispersion and more consistency in the year-to-year events as the rainfall rates increase beyond 10 mm d^{-1} (Figures 9b and 9c).

Impact of climate change on winter wheat production

The main causes of wheat yield increase in the irrigated regions of Dashte Abbas (21%) (Figure 10a) are as follows: a general decrease in the diurnal temperature range (by 2°C) as minimum temperature increases (Figures 4e–4h) as well

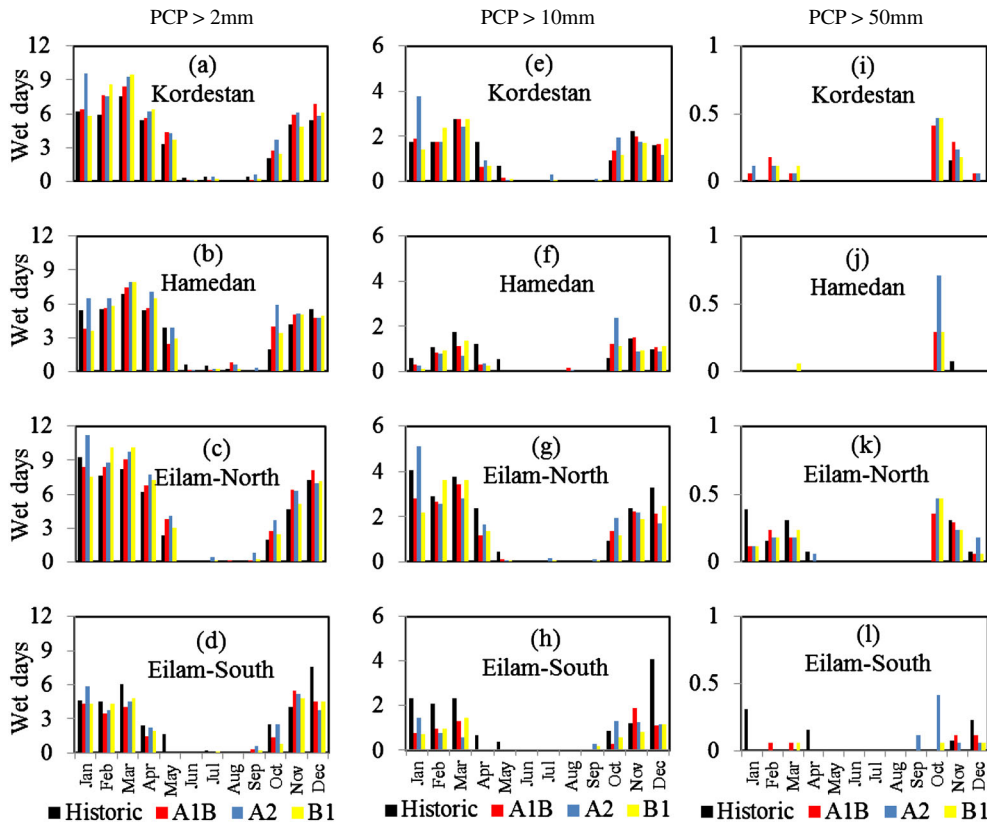


Figure 7. Comparison of the number of wet days ($> 2 \text{ mm d}^{-1}$ left column, $> 10 \text{ mm d}^{-1}$ middle column and $> 50 \text{ mm d}^{-1}$ right column) between the historical (1985–2005) and the future scenarios (2020–2040) for four selected subbasins

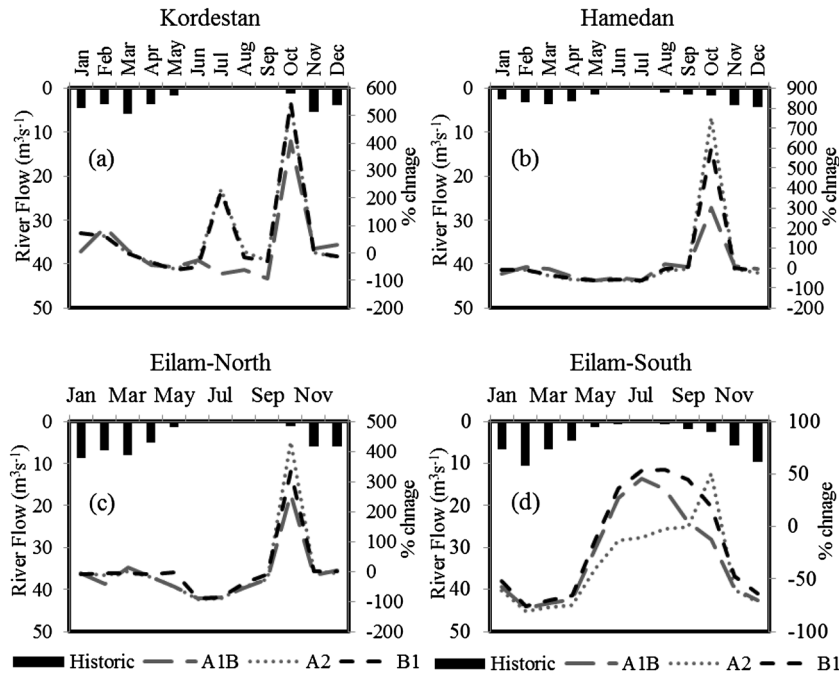


Figure 8. Comparison of average monthly river flow ($\text{m}^3 \text{ s}^{-1}$) between the historical (1985–2005) and the future scenarios (2020–2040) for four selected subbasins

as an increase in the blue water resources by 25% (Figures 5a–5d). In the rain-fed areas (Figure 10b), the wheat yield increases in Dashte Abbas (38%) because it sees a large increase in the precipitation (60%), resulting in an increase in the soil water (25%) (Figures 5e–5h). In Arayez,

B1 scenario shows a decrease in yield of 5% mostly because of a decrease in the predicted soil water by 25%. The KRB could in the future be an important wheat surplus region able to fill the shortfalls from other provinces through virtual water trade as discussed by Faramarzi *et al.* (2010b).

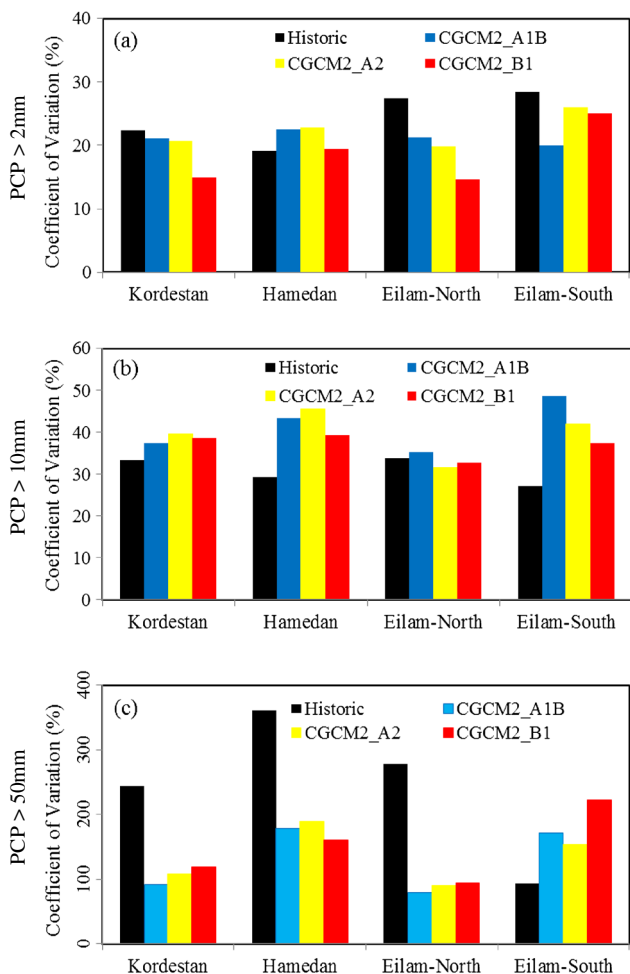


Figure 9. CV of the number of wet days with (a) precipitation >2 mm, (b) precipitation >10 mm and (c) precipitation >50 mm for four selected subbasins across the KRB.

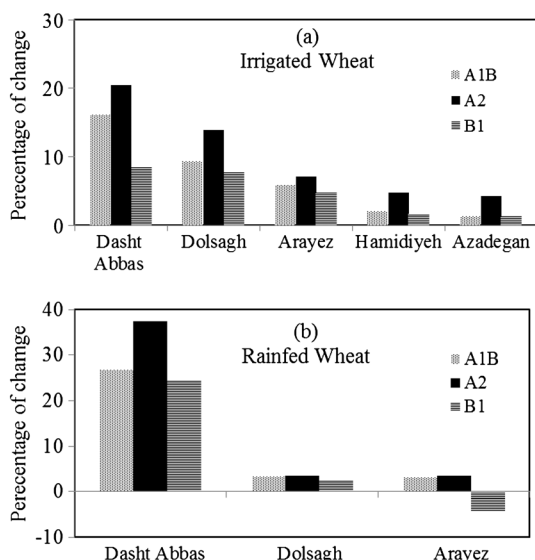


Figure 10. Anomaly graphs of irrigated and rain-fed wheat yields in the future for five major agricultural lands in the lower KRB.

Study limitations

It must be pointed out that in this study, the predictions of hydrological components for the future was based on

the use of the same land cover as the historic times. This may have under estimated the AET as denser vegetation and, consequently, larger AET may result from higher temperature and CO₂ concentration in the future (Abbaspour *et al.*, 2009). In addition, this study does not consider any changes in the soil parameters in the future. Land use changes such as urbanization, reforestation and deforestation change surface properties, which in turn affect partitioning of rainfall into runoff and infiltration. Also, soil erosion, which is widespread in Iran, may change soil properties and lead to different responses of soil in partitioning the infiltrated water between AET, soil moisture and deep aquifer recharge (Setegn *et al.*, 2011). Therefore, an advanced study of climate change impact assessment while considering the land cover and soil parameter changes would increase the confidence on the projected results.

There is a large variability in the prediction of future climate scenario among different GCM models. In this study, we used one GCM with three different scenarios. Future studies should use a larger ensemble of GCMs and development scenarios.

Another source of uncertainty in this study is from future development plans of the region and construction of water management systems and irrigation networks. Many dams have been constructed in Iran in the past years. Dams and reservoirs can substantially change the hydrology of a region. Therefore, our projected results must be viewed keeping in mind the assumptions of this study.

SUMMARY AND CONCLUSION

The Challenge Program on Water and Food recognizes Karkheh as a benchmark river basin to address severe environmental degradation in the basin through the underlying social and biophysical causes (Oweis *et al.* 2009). The research work that the themes cover obtains geographical definition by focusing on nine river basin spread across the developing world. The procedures used in this study are general and could be applied to all the Challenge Program on Water and Food benchmark basins.

In this study, we quantified the impact of climate change on spatial variation of water availability, drought events and wheat yield across the KRB by building a SWAT model of the region. The model used wheat yield and river discharge data for calibration and validation. A newly developed program called CCDC was used to determine the frequency and length of critical precipitation, maximum temperature and soil moisture periods. By using parallel SUFI2, the SWAT model was calibrated and accounted for different sources of uncertainties, including input data, conceptual model and parameter uncertainties. A total of 26 flow and crop yield parameters were calibrated with the most sensitive ones shown in Table II. Considering the large scale of the basin and lack of water use data, the results are very satisfactory and provide notable insight into the water availability, drought events and wheat yield and associated uncertainties in KRB.

We found that the northern part of KRB (Upper Karkheh) will face a better situation in the future in water components like precipitation, blue water and green water resources. In the southern part of the Basin (lower Karkheh), where much of the agricultural lands are located, a less favorable climate and water availability situation than the historical period will ensue.

Although precipitation in the future for lower Karkheh will not decline, changes in the interannual distribution of precipitation will cause an increase in the frequency and average length of the critical continuous periods for precipitation, maximum temperature and soil water in the future.

Finally, we observed a general increase in winter wheat yields in the rain-fed as well as the irrigated lands, which should be noted for the future planning of the region.

ACKNOWLEDGEMENTS

The authors express their sincere thanks to Eawag Partnership Program for the opportunity of a collaboration. Special thanks are given to Ms. Monireh Faramarzi, Mr. Majid Ehtiat and Ms. Neda Naghsh Nilchi in providing information, data and useful references and comments.

REFERENCES

- Abbaspour KC. 2011. User manual for SWAT-CUP, SWAT calibration and uncertainty analysis programs, 103 pp., Eawag: Swiss Federal Institute of Aquatic Science and Technology., Duebendorf, Switzerland (<http://www.eawag.ch/forschung/siam/software/swat/index>).
- Abbaspour KC, Johnson A, van Genuchten MT. 2004. Estimating uncertain flow and transport parameters using a sequential uncertainty fitting procedure. *Vadose Zone Journal* **3**(4): 1340–1352.
- Abbaspour KC, Yang J, Maximov I, Siber R, Bogner K, Mieleitner J, Zobrist J, Srinivasan R. 2007. Modelling hydrology and water quality in the prealpine/alpine 2007. Modelling hydrology and water quality in the prealpine/alpine Thur watershed using SWAT. *Journal of Hydrology* **333**: 413–430.
- Abbaspour KC, Faramarzi M, Ghasemi SS, Yang H. 2009. Assessing the impact of climate change on water resources in Iran. *Water Resources Research* **45**: W10434. doi:10.1029/2008WR007615.
- Adams RM, Hurd BH, Lenhart S, Leary N. 1998. Effects of global climate change on agriculture: an interpretative review. *Climate Research* **11**: 19–30.
- Ahmad MD, Giordano M. 2010. The Karkheh River Basin: the food basket of Iran under pressure. *Water International* **35**(5): 522–544.
- Ahmad MD, Islam MDA, Masih I, Muthuwatta L, Karimi P, Tural H. 2009. Mapping basin-level water productivity using remote sensing and secondary data in the Karkheh River Basin, Iran. *Water International* **34**(1): 119–133.
- Arnold JG, Srinivasan R, Mutiah RS, Williams JR. 1998. Large area hydrologic modeling and assessment - Part I: Model development. *Journal of the American Water Resources Association* **34**(1): 73–89.
- Arnold JG, Srinivasan R, Mutiah RS, Allen PM. 1999. Continental scale simulation of the hydrologic balance. *Journal of the American Water Resources Association* **35**(5): 1037–1052.
- Beyene T, Lettenmaier DP, Kabat P. 2010. Hydrologic impact of climate change on the Nile River Basin: implications of the 2007 IPCC scenarios. *Climatic Change* **100**: 433–461.
- Easterling DR, Meehl GA, Parmesan C, Changnon SA, Karl TR, Mearns O. 2000. Climate extremes: Observation, Modeling and impacts. *Science* **289**: 2068–2074.
- Falkenmark M, Rockström J. 2006. The new blue and green water paradigm: Breaking new ground for water resources planning and management. *Journal of Water Resources Planning and Management ASCE* **132**(3): 129–132.
- Farahani H, Oweis T. 2008. Chapter I Agricultural Water Productivity in Karkheh River Basin. In: Oweis T, Farahani H, Qadir M, Anthofer J, Siadat H, Abbasi F, Bruggeman A. (Eds). *Improving On-farm Agricultural Water Productivity in the Karkheh River Basin*. Research Report no. 1: A Compendium of Review Papers. ICARDA: Aleppo, Syria. IV +103 pp.
- Faramarzi M, Abbaspour KC, Schulin R, Yang H. 2009. Modelling blue and green water resources availability in Iran. *Hydrological Processes* **23**: 486–501.
- Faramarzi M, Yang H, Schulin R, Abbaspour KC. 2010a. Modeling wheat yield and crop water productivity in Iran: Implications of agricultural water management for wheat production. *Agricultural Water Management* **97**: 1861–1875.
- Faramarzi M, Yang H, Mousavi J, Schulin R, Binder CR, Abbaspour KC. 2010b. Analysis of Intra-country virtual water trade strategy to alleviate water scarcity in Iran. *Hydrology and Earth System Sciences* **14**: 1417–1433.
- Food and Agriculture Organization (FAO). 1995. The digital soil map of the world and derived soil properties, version 3.5 (CD-ROM), Rome.
- Gassman PW, Reyes M, Green CH, Arnold JG. 2007. The Soil and Water Assessment Tool: Historical development, applications, and future directions. *Transaction of ASABE* **50**(4): 1211–1250.
- IPCC, 2007. Climate change 2007: the physical science basis. In: Solomon S, Qin D, Manning M, Chen Z, Marquis M, Averyt KB, Tignor M, Miller HL (Eds.), *Contribution of Working Group I to the Fourth Assessment Report of the Intergovernmental Panel on Climate Change*. Cambridge University Press: Cambridge, United Kingdom and New York, NY, USA, p. 996.
- IPCC SRES. 2000. Nakićenović N., and Swart, R., ed., Special Report on Emissions Scenarios: A special report of Working Group III of the Intergovernmental Panel on Climate Change, Cambridge University Press, ISBN 0-521-80081-1, <http://www.ipcc.ch/pdf/special-reports/spm/sres-en.pdf>.
- Iran Water & Power Resources Development Co. 2010. Systematic studies of Karkheh River Basin (Available in Persian).
- Jarvis A, Reuter HI, Nelson A, Guevara E. 2008. Hole-filled SRTM for the globe Version 4, available from the CGIAR-CSI SRTM 90m Database (<http://srtm.csi.cgiar.org>).
- Keshavarz A, A Sh, Haydari N, Pouran M, Farzaneh EA. 2005. Water allocation and pricing in agriculture of Iran. In: *Water Conservation, Reuse, and Recycling: proceeding of an Iranian American Workshop*. The National Academies Press: Washington, DC; 153–172.
- Liu J, Fritz S, van Wesenbeeck CFA, Fuchs M, Obersteiner M, Yang H. 2009. A spatially explicit assessment of current and future hotspots of hunger in Sub-Saharan Africa in the context of global change. *Global and Planetary Change* **64**: 222–235.
- Lobel DB. 2007. Changes in diurnal temperature range and national cereal yields. *Agriculture and Forest Meteorology* **145**: 229–238.
- Mahab Ghods Consulting Engineer Co. 2009. Systematic planning of Karkheh Watershed: studying the water consumption of demand sectors, Vol. 3 (Available in Persian).
- Marjanizadeh S, de Fraiture C, Loiskandl W. 2010. Food and water scenarios for the Karkheh River Basin, Iran. *Water International* **35**(4): 409–424.
- Masih I, Uhlenbrook S, Maskey S, Ahmad MD. 2010. Regionalization of a conceptual rainfall-runoff model based on similarity of the flow duration curve: A case study from the semi-arid Karkheh basin, Iran. *Journal of Hydrology* **391**: 188–201.
- Milly PCD, Dunne KA, Vecchia VV. 2005. Global pattern of trends in stream flow and water availability in changing climate. *Nature* **438**(17): 347–350. doi:10.1038/nature04312.
- Ministry of Energy of Iran. 1998. An Overview of National Water Planning of Iran. Tehran, Iran (Available in Persian).
- Mishra AK, Singh VP. 2011. Drought modeling-A review. *Journal of Hydrology* **357**(3–4): 349–367.
- Moriasi DN, Arnold JG, Van Liew MW, Bingner RL, Harmel RD and Veith TL. 2007. Model evaluation guidelines for systematic quantification of accuracy in watershed simulations. *Transactions of the ASABE* **50**(3): 885–900.
- Mousavi SF. 2005. Agricultural drought management in Iran. In: *Water Conservation, Reuse, and Recycling: Proceeding of an Iranian American Workshop*. The National Academies Press: Washington, D.C.; 107–113.
- Muthuwatta LP, Mobin-ud-Din A, Bos MG, Rientjes, THM. 2010. Assessment of Water Availability and Consumption in the Karkheh River Basin, Iran—Using Remote Sensing and Geo-statistics. *Water Resources Management* **24**: 459–484.
- Myneni RC, Keeling CD, Tucker CJ, Asrar G, Nemani RR. 1997. Increased plant growth in the northern high latitudes from 1981 to 1991. *Nature* **386**: 698–702.

IMPACT OF CLIMATE CHANGE ON WATER RESOURCES OF KARKHEH RIVER BASIN

- Nash JE, Sutcliffe JV. 1970. River flow forecasting through conceptual models Part 1 – A discussion of principles. *Journal of Hydrology* **10**(3): 282–290.
- Neitsch SL, Arnold JG, Kiniry JR, Williams JR, King KW. 2002. Soil and Water Assessment Tool. Theoretical documentation: Version 2009, TWRITR-191. Texas Water Resources Institute, College Station, TX.
- Oweis T, Siadat H, Abbasi F, project team. 2009. CPWF project report: Improving on farm agricultural water productivity in the Karkheh River Basin. PN8 Completion Report: ICARDA and CPWF.
- Rouholahnejad E, Abbaspour KC, Vejdani M, Srinivasan R, Schulin R, Lehmann A. 2012. Parallelization framework for calibration of hydrological models. *Environmental Modelling & Software* **31**: 28–36.
- Salajegheh A, Razavizadeh S, Khorasani N, Hamidifar M, Salajegheh S. 2011. Land use changes and its effects on water quality (case study: Karkheh River Basin). *Journal of Environmental Studies* **37**(58): 22–25.
- Schuol J, Abbaspour KC, Srinivasan R, Yang H. 2008a. Estimation of freshwater availability in the West African Sub-continent using the SWAT hydrologic model. *Journal of Hydrology* **352**: 30–49.
- Schuol J, Abbaspour KC, Srinivasan R, Yang H. 2008b. Modeling blue and green water availability in Africa at monthly intervals and subbasin level. *Water Resources Research* **44**: W07406. doi:10.1029/2007WR006609.
- Setgen SG, Rayner D, Melesse AM, Dargahi B. 2011. Impact of climate change on the hydroclimatology of Lake Tana Basin, Ethiopia. *Water Resources Research* **47**: W04511. doi:10.1029/2010WR009248.
- Srinivasan R, Arnold JG, Jones CA. 1998. Hydrologic modeling of the United States with the Soil and Water Assessment Tool. *International Journal of Water Resources Development* **14**(3): 315–325.
- Tao F, Zhang Z, Liu J, Yokozawa M. 2009. Modelling the impact of the weather and climate variability on crop productivity over a large area: a new super-ensemble-based probabilistic projection. *Agricultural and Forest Meteorology* **149**: 1266–1278.
- Vörösmarty CJ, Green PJ, Salisbury J, Lammers RB. 2000. Global water resources: vulnerability from climate change population growth. *Science* **289**: 284–288.
- Wang J, Wang E, Liu DL. 2011. Modeling the impact of climate change on wheat yield and field water balance over the Murray-Darling Basin in Australia. *Theoretical and Applied Climatology* **104**: 285–300. doi: 10.1007/s00704-010-0343-2.
- Wilby RL, Wigley TML. 1997. Downscaling general circulation model output: a review of methods and limitations. *Progress in Physical Geography* **21**: 530–548.
- Xiao G, Zhang Q, Wang R, Yao Y, Zhao H, Bai H. 2010. Impact of temperature increase on the yield of winter wheat at low and high altitudes in semiarid northwestern China. *Agricultural Water Management* **97**: 1360–1364.
- Yang H, Reichert P, Abbaspour KC, Zehnder AJB. 2003. A water resources threshold and its implications for food security. *Environmental Science and Technology* **37**: 3048–3054.